Effects of residual particles and multiply charged particles of a polystyrene latex particle on the particle filtration efficiency of a medical face masks

Papol Sardyoung[1, *], Panich Intra[2], Theerachot Lawong[3] and Wisanapat Rattanachan[4]
[1] Department of Industrial Electrical Technology, Faculty of Industrial Technology Thepsatri Rajabhat University, Thale Chupsorn, Mueang Lopburi, Lopburi 15000, Thailand
[2] Research Unit of Applied Electric Field in Engineering College of Integrated Science and Technology, Rajamangala University of Technology Lanna, Chang Phueak, Mueang Chiang Mai, Chiang Mai, 50220, Thailand
[3] Master of Engineering Program in Electrical Engineering, Rajamangala University of Technology Lanna, Chang Phueak, Mueang Chiang Mai, Chiang Mai, 50220, Thailand
[4] Master of Engineering Program in Environment Engineering, Chiang Mai University, Suthep, Mueang Chiang Mai, Chiang Mai 50220, Thailand
***Corresponding Author E-mail:** papolxyz@gmail.com
Received: Sep 25, 2024; **Revised:** Dec 20, 2024; **Accepted:** Jan 17, 2025

Abstract

The objective of this study is to elucidate the impact of residual particles and multiply charged particles of polystyrene latex (PSL) particles on the particle filtration efficiency of a medical face mask. Adhering to the ASTM F2299 test methodology, this investigation employed a PSL particle (Thermo ScientificTM Dri-CalTM) with a diameter of 100 nanometers and a geometric standard deviation of approximately 1.6%. The scanning mobility particle sizer (SMPS) was utilized to ascertain the size distribution of PSL particles both upstream and downstream of the test face mask, thereby determining the particle filtration efficiency of the face mask for residual particles and multiply charged particles at various PSL particle-to-DI water ratios. The PSL particle-to-DI water ratios employed in this study were 10, 20, and 100 drops per 200 mL, respectively. The findings revealed that PSL suspension residual particles with a mobility diameter less than 60 nanometers, as well as multiple charged particles with a mobility diameter exceeding 100 nanometers, introduced complexity to purportedly monodisperse particle aerosols. An increase in PSL suspension concentration resulted in a heightened relevance of the residual peak. At elevated concentrations, PSL multiply charged particles became discernible in the size distribution. Furthermore, it was demonstrated that as the PSL particle-to-DI water ratios increased, the particle filtration efficiency of the test face mask diminished for both single charged particles and multiply charged particles (+2, +3, +4, and +5).

Keywords: Residual particle, Multiply charged particle, Polystyrene latex particle, Filtration efficiency, Respirator

1. Introduction

Facepiece respirators, medical face masks, and other face coverings are employed to purify the airstream entering or exiting the wearer's respiratory system in various environments, including industrial, healthcare, and public health settings [1],[2]. The efficacy of such face coverings is primarily determined by the filtration media employed and the seal formed with the wearer's face. While total inward leakage assessment should be performed on a case-by-case basis, filtration efficiency can be quantified using standardized and universally applicable test procedures. During the COVID-19 pandemic in Thailand [3], a shortage of medical equipment, particularly medical face masks, led to significant price increases. It was discovered that many certified medical face masks that had not met certification standards were being sold on the market. Consequently, the particle filtering efficiency of non-standard masks is significantly lower compared to that of standard medical face masks [4]. Medical face masks, such as those governed by the ASTM F2299 test method [5] and the ASTM F2100 test method [6], were frequently utilized to mitigate the transmission of airborne respiratory infections during the COVID-19 pandemic.

The ASTM F2299 standard has been employed in the United States to assess the initial efficacy of materials utilized in medical face masks in terms of particulate penetration. This method utilizes monodisperse polystyrene latex (PSL) particles, specifically latex spheres, in the size range of 0.1 to 5.0 μm, along with airflow test velocities ranging from 0.5 to 25 cm/s. The PSL particles exhibit monodisperse properties, with a geometric standard deviation (GSD) approximately equal to 1. The test procedure evaluates filtration efficiency by comparing the particle count in the feed stream (upstream) to that in the filtrate (downstream).

However, in practical applications, residual particles and multiply charged particles can complicate the PSL particles scenario. The ideal monodisperse size distribution anticipated for PSL particles is rarely achieved in real-world scenarios. Aerosols typically contain a substantial number of small residual particles and multiply charged

particles, in addition to PSL particles. These particles can potentially impact the particle filtration efficiency of medical face masks, thereby affecting the measurement of upstream and downstream particle number concentrations using a light scattering particle counter.

Despite the potential impact of residual particles and multiply charged particles on particle filtration efficiency, extensive research in the literature has not focused on the effects of these particles on the particle filtration efficiency of medical face masks. Therefore, the effects of residual particles and multiply charged particles of the PSL particle on the particle filtration efficiency of face masks were experimentally investigated in this work to enhance the ASTM F2299 test method for determining the filtration efficiency of PSL particles in medical face masks. This study utilized a PSL particle (Thermo ScientificTM Dri-CalTM) with a diameter of 100 nm and a geometric standard deviation of approximately 1.6%, as specified in the ASTM F2299 test method. Subsequently, the particle filtration efficiency of face masks was evaluated for residual particles and multiply charged particles at various PSL particle-to-DI water ratios (10, 20, and 100 drops per 200mL, respectively).

2. Materials and Methods

Figure 1 shows the SEM image of the PSL particles that used in this study. In this study, five FDA-approved medical face masks from Thai manufacturers were selected based on availability from suppliers in Thailand. **Figure 2(a)** depicts the experimental setup employed for measuring the size distribution of the PSL particles. The setup comprises an aerosol atomizer, a filtered air supply, concentration adjustment valves, a high-efficiency particulate-free air (HEPA) filter, a diffusion dryer, an aerosol neutralizer, an electrostatic classifier, and an ultrafine condensation particle counter (UCPC). PSL particles were generated using an aerosol atomizer (Model 3076, TSI Inc., St. Paul, MN, USA) to atomize a PSL solution. PSL particles (Thermo Scientific™ Dri-Cal™) with a diameter of 100 nm and a geometric standard deviation of approximately 1.6% were certified by the National Institute of Standards and Technology (NIST), USA.

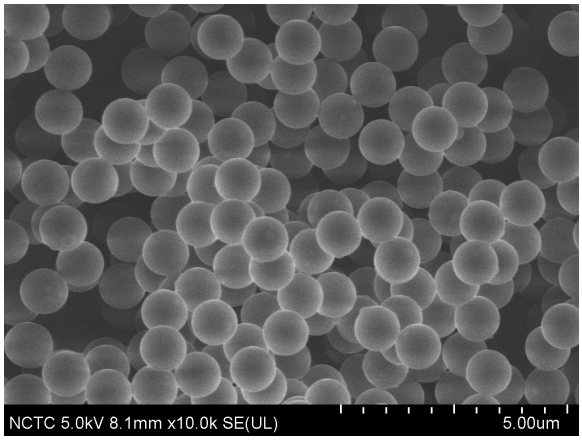

Figure 1 SEM image of the PSL particles used in this study

In this investigation, the ratio of PSL particles to DI water was 10, 20, and 100 drops per 200 mL, respectively. The diffusion dryer (Model 3062, TSI Inc., St. Paul, MN, USA) was utilized to dry the wet PSL particles generated by the aerosol atomizer to a relative humidity of less than approximately 30 % RH. The number concentration of PSL particles could be adjusted by manipulating the concentration adjustment valves and a HEPA capsule filter (Model 1602051, TSI Inc., St. Paul, MN, USA). PSL particles were subsequently introduced into the SMPS, which consisted of an aerosol neutralizer, an electrostatic classifier (Model 3082, TSI Inc., St. Paul, MN, USA) equipped with a long-differential mobility analyzer (long DMA, model 3081, TSI Inc., St. Paul, MN, USA), and a universal condenser particle counter (UCPC, Model 3788, TSI Inc., St. Paul, MN, USA). The particles were neutralized and brought to Boltzman charge equilibrium using a soft X-ray aerosol neutralizer (Model 3088, TSI Inc., St. Paul, MN, USA). Subsequently, the SMPS was employed to ascertain the size distribution of PSL particles, with a mobility diameter range spanning 10 to 700 nm.

The experimental setup for evaluating the particle filtration efficiency of the test face mask is depicted in **Figure 2(b)**. To achieve the optimal aerosol flow rate, neutralized PSL particles from the aerosol generator were supplied to the mixing chamber at a flow rate of approximately 1.5 L/min. Simultaneously, filtered air was introduced at a flow rate of approximately 7.4 L/min to facilitate the mixing and dilution of PSL particles with clean air. For a test area of 17.8 cm2, an aerosol flow rate of approximately 11.3 L/min was employed, resulting in a Reynolds number of approximately 332.48 and a Stokes number of approximately 0.41. PSL particles were propelled into a test chamber with a diameter of 4.76 cm and a length of 100 cm, positioned 10 duct diameters (9.52 cm) from the particle inlet. The particle sampling probe utilized for measuring upstream particle concentration was situated two duct diameters (9.52 cm) prior to the material specimen, while the particle sampling probe employed for measuring downstream particle concentration was situated three duct diameters (14.28 cm) behind the material specimen. The diameter of both sample probes was 1.1 cm. In this experiment, isokinetic sampling was employed, and the differential pressure across the test face mask was measured using a manometer (Model 8380, TSI Inc., St. Paul, MN, USA). Subsequently, the SMPS was utilized to ascertain the particle filtration efficiency of the test face mask by measuring the size distribution of the particles. Both upstream and downstream of the test face mask, PSL particles are present. The particle filtration efficiency, η , is the converse of filter penetration, P , and given by Eq. (1). willeke [7] and Hinds [8]

$$\eta = 100 - P \quad (1)$$

Penetration was calculated as Eq. (2). willeke [7] and Hinds [8]

$$P = \left(\frac{c_{down}}{c_{up}}\right) \times 100 \qquad (2)$$

where c_{up} and c_{down} are upstream and downstream particle number concentrations of the test face mask.

In this study, the particle filtration test was conducted three times per piece, and the average value for each piece was determined. Subsequently, the average of the five pieces was calculated. For this test, the temperature and relative humidity within the test chamber were maintained at approximately 25 ± 5°C and 55±10%RH, respectively. **Table 1** presents the ranges and values of the variables studied.

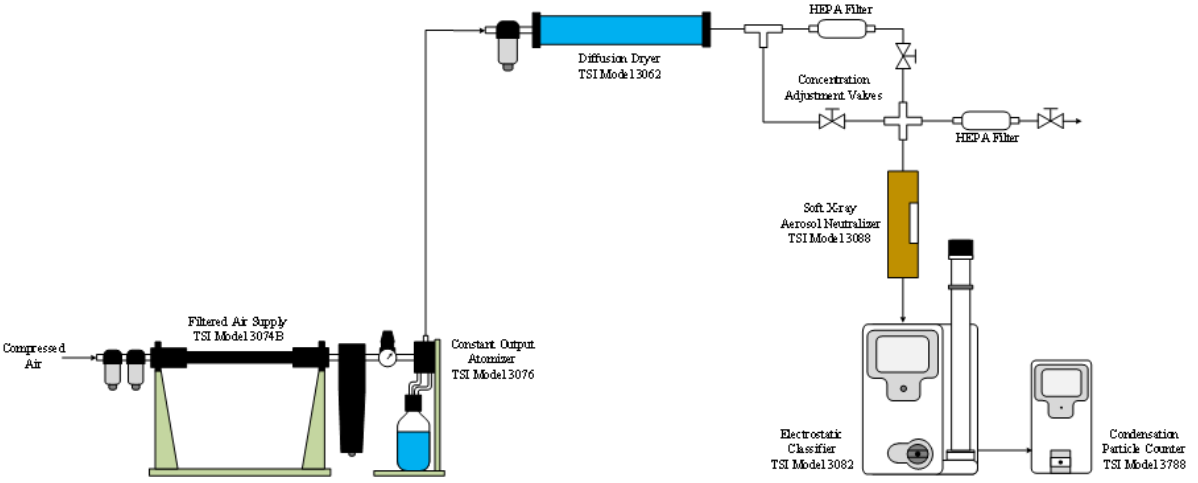

(**a**)

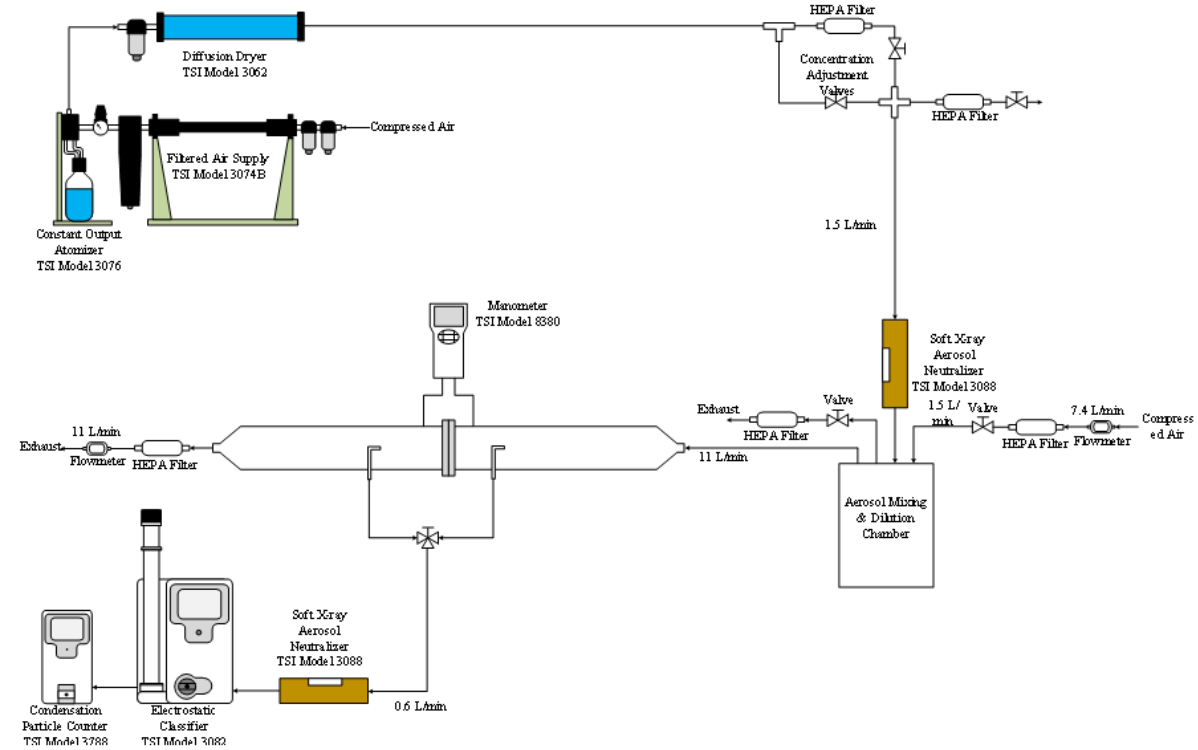

(**b**)

Figure 2 Experimental setup for evaluating the effects of residual particles and multiply charged particles of the PSL particle on the particle filtration efficiency of face mask. (**a**) Particle size distribution of PSL particles (**b**) Filtration efficiency of PSL particles

Table 1 Ranges and values of variables investigated

Variable	Range
Particle	Polystyrene Latex spheres
Particle number concentration	0.1 μm
Particle size	$0.1–1.7 \times 10^4$ particles/cm^3
Filter Test Area	17.8 cm3
Flow rate	11.3 L/min
Face velocity	10.6 cm/s
Operating relative humidity	55 ± 10%RH
Operating pressure	1atm
Operating temperature	25 ± 5°C

3. Results and Discussion

Figure 2 presents the particle size distribution of blank water and PSL particles in DI water at concentrations of 10, 20, and 100 drops per 200 mL, respectively. Consequently, a completely monodisperse particle distribution cannot be achieved from a PSL suspension. PSL suspension residues, particles with a mobility diameter less than 60 nanometers, and multiply charged particles, particles with a mobility diameter greater than 100 nanometers, introduce complexity to ostensibly monodisperse particle aerosols. Even in dilute mixtures, multiply charged particles can be detected. Furthermore, the aerosol always contains a substantial number of small residual particles. The mean size of the residual particle was approximately 28.9, 34.3, 29.4, and 32.2 nanometers, with geometric standard deviations of approximately 1.49, 1.44, 1.49, and 1.52, respectively, for blank water, 10 drops per 200 mL, 20 drops per 200 mL, and 100 drops per 200 mL, respectively. The surfactant added to commercial PSL solutions to prevent PSL coagulation is evident in these residual particles. Increasing the PSL concentration in suspension elevates the prominence of the residual peak. PSL multiply charged particles with charges of +2, +3, +4, +5, and so on become noticeable in the size distribution at higher concentrations. As presented in **Table 2**, the mean particle size for 10 drops in 200 mL was approximately 103.3, 143.5, 176.9, 248.1, and 365.1 nanometers. The particle number concentration was approximately 333.0, 92.5, 46.1, 31.0, and 6.65 particles per cubic centimeter. The geometric standard deviation for each particle size distribution (for +1, +2, +3, +4, and +5) was approximately 1.07, 1.07, 1.06, 1.10, and 1.10, respectively.

The mean particle size for 20 drops in 200 mL was approximately 103.7, 141.8, 174.0, 223.8, and 358.8 nanometers. The particle number concentration was approximately 419.0, 157.6, 64.1, 61.3, and 29.3 particles per cubic centimeter. The geometric standard deviation for each particle size distribution (for +1, +2, +3, +4, and +5) was approximately 1.07, 1.08, 1.05, 1.11, and 1.19, respectively.

The mean particle size for 100 drops in 200 mL was approximately 103.2, 143.8, 174.5, 204.8, and 297.8 nanometers. The particle number concentration was approximately 1220, 608.4, 334.5, 193.9, and 573.0 particles per cubic centimeter. The geometric standard deviation for each particle size distribution (for +1, +2, +3, +4, and +5) was approximately 1.07, 1.08, 1.05, 1.04, and 1.30, respectively. It is noteworthy that nebulized aerosol particles, such as those produced in ASTM standards [5] and [6], are initially even more heavily charged. This is because of the mechanical nebulization process and the fact that nebulized droplets are larger than dry particles. Furthermore, it is important to recognize that the electrical charge of natural aerosol particles is common. Consequently, nebulized particles must be "neutralized" to a state of equilibrium. A Boltzmann distribution represents the equilibrium state, not zero charge per particle. A substantial concentration of positive and negative air ions is generated by all neutralizers. The neutralizer interacts with these ions until a charge distribution equilibrium is reached. Notably, the ASTM F2299 test method [5] suggests but does not necessitate charge neutralization. Previously, the United States Food and Drug Administration (US FDA) provided recommendations suggesting the use of unneutralized particles with the ASTM test method. This approach was justified by the significant role of electrostatic deposition in the initially high filtration efficiency, resulting in the lowest efficiency for uncharged particles.

Table 2 Multiply charged particles, mean size, number concentration and geometric standard deviation of PSL particles at different PSL particle to DI water ratios

Ratio of PSL	P	Mean Size (nm)	Number Concentration (particles/cm^3)	Geometric Standard Deviation
10 drop/200 mL	+1	103.3	333	1.07
	+2	143.5	92.5	1.07
	+3	176.9	46.1	1.06
	+4	248.1	31	1.1
	+5	365.1	6.65	1.1
20 drop/200 mL	+1	103.7	419	1.07
	+2	141.8	157.6	1.08
	+3	174.9	64.1	1.05
	+4	223.8	61.3	1.11
	+5	358.8	29.3	1.19

Table 2 Multiply charged particles, mean size, number concentration and geometric standard deviation of PSL particles at different PSL particle to DI water ratios (cont.)

Ratio of PSL	P	Mean Size (nm)	Number Concentration (particles/cm^3)	Geometric Standard Deviation
100 drop/200 mL	+1	103.2	122	1.07
	+2	143.8	608.4	1.08
	+3	174.5	334.5	1.05
	+4	204.8	193.9	1.04
	+5	207.8	573	1.3

Figure 3 presents the measured particle size distribution at the upstream and downstream of the respirator filter for blank water, 10 drops per 200 mL, 20 drops per 200 mL, and 100 drops per 200 mL, respectively.

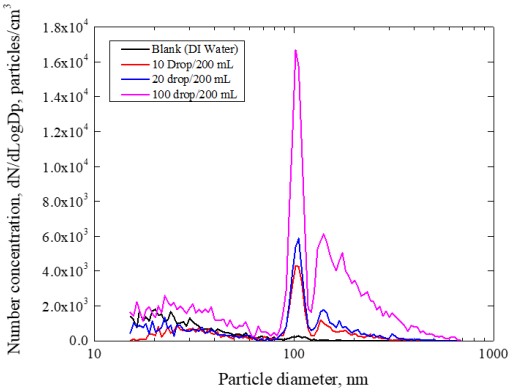

Figure 3 Particle size distribution of PSL particles

As indicated in **Table 3**, the upstream particle concentration of blank water, 10 drops per 200 mL, 20 drops per 200 mL, and 100 drops per 200 mL was approximately 595.4, 256.2, and 369.0 particles per cubic centimeter, respectively. Conversely, the downstream particle concentration of blank water, 10 drops per 200 mL, 20 drops per 200 mL, and 100 drops per 200 mL was approximately 5.78, 8.26, and 11.9 particles per cubic centimeter, respectively. The upstream and downstream particle concentrations can be utilized to calculate the particle filtration efficiency of the test face mask [9]. The particle filtration efficiency of the test face mask was approximately 99.03%, 96.77%, and 96.77% for blank water, 10 drops per 200 mL, and 20 drops per 200 mL, respectively. The particle filtration efficiency of the test face mask was approximately 96.21% for 100 drops per 200 mL.

Table 3 Mean size, number concentration, geometric standard deviation and filtration efficiency of residual particles at different PSL particle to DI water ratios

	Size (nm)	Standard Deviation	Particle Concentration (particles/cm^3)	Particle Concentration (particles/cm^3)	Efficiency (%)
Blank (DI water)	28.9	1.49	595.4	5.78	99.03
10 drop/200 mL.	34.3	1.44	256.2	8.26	96.77
20 drop/200 mL.	29.4	1.49	369	11.9	96.77
100 drop/200 mL.	32.2	1.52	1010	38.2	96.21

Figure 4 demonstrates the particle filtration efficiency of the test face mask for particle sizes of +1, +1 - +5, and +1 - +5, along with the corresponding residual particles. It is evident that as the particle-to-blank water ratios increase, the particle filtration efficiency of the test face mask diminishes for both single-charged particles and multiply charged particles (+2, +3, +4, and +5). At a drop rate of 10 drops per 200 mL, the particle filtration efficiency of the test face mask ranges from approximately 99.41% to 98.53% for particles of sizes +1, +1 - +5, and +1 - +5, respectively. For a drop rate of 20 drops per 200 mL, the particle filtration efficiency ranges from approximately 98.89% to 98.13% for particles of sizes +1, +1 - +5, and +1 - +5, respectively. Finally, for a drop rate of 100 drops per 200 mL, the particle filtration efficiency ranges from approximately 98.06% to 98.02% for particles of sizes +1, +1 - +5, and +1 - +5, respectively.

Furthermore, the particle charge significantly influences the filtration efficiency. Most high-performance respirators utilize electret materials (materials with permanent dipoles) to induce image charges on particles, thereby enhancing particle capture. However, for particles with aerodynamic or mobility dimensions of 100 to 300 nm, mechanical capture (diffusion, impaction, and interception) becomes ineffective.

It is noteworthy that optical particle counters were employed as detectors in the ASTM F2299 test method. The light scattering effectiveness of small particles decreases rapidly with particle size, leading to a compromised responsiveness of optical particle counters for smaller particles. Consequently, the sensitivity of optical particle counters used for particle filtration efficiency testing must be periodically validated and tested [10].

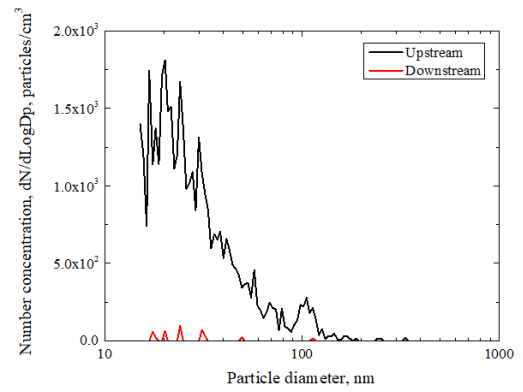

(**a**) Blank water

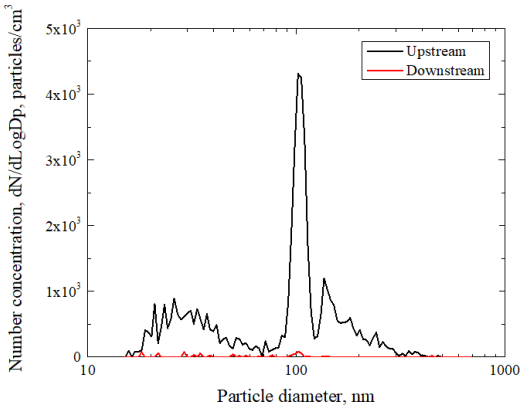

(**b**) 10 drop/200 mL

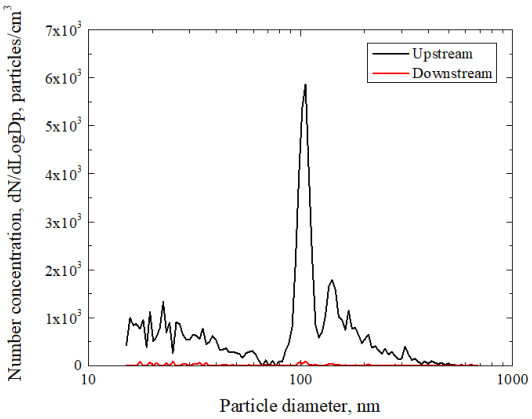

(**c**) 20 drop/200 mL

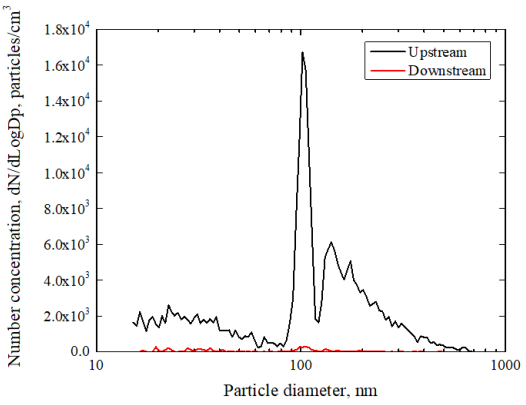

(**d**) 100 drop/200 mL

Figure 4 Particle size distribution at upstream and downstream of respirator filter

4. Conclusion

Figure 5 presents the particle filtration efficiency of the test face mask for particle sizes of +1, +1 - +5, and +1 - +5, along with the corresponding residual particles. It is evident that as the particle-to-blank water ratios increase, the particle filtration efficiency of the test face mask diminishes for both single-charged particles and multiply charged particles (+2, +3, +4, and +5). At a drop rate of 10 drops per 200 mL, the particle filtration efficiency ranges from approximately 99.41% to 98.53% for particles of sizes +1, +1 - +5, and +1 - +5, respectively. For a drop rate of 20 drops per 200 mL, the particle filtration efficiency ranges from approximately 98.89% to 98.13% for particles of sizes +1, +1 - +5, and +1 - +5, respectively. Finally, for a drop rate of 100 drops per 200 mL, the particle filtration efficiency ranges from approximately 98.06% to 98.02% for particles of sizes +1, +1 - +5, and +1 - +5, respectively.

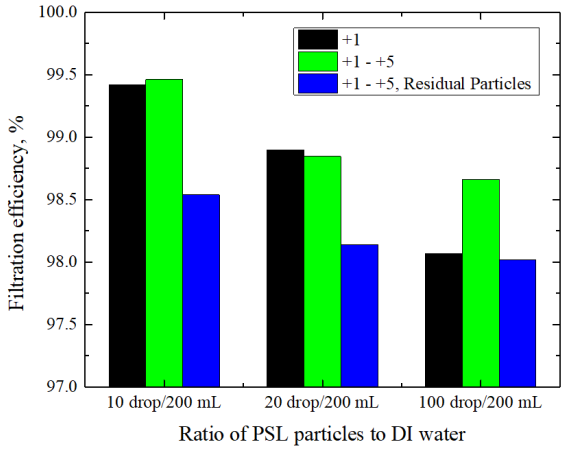

Figure 5 Filtration efficiency of test face mask for +1 , +1 - +5 and +1 - +5 and residual particles

Additionally, the particle charge significantly influences the filtration efficiency. Most high-performance respirators utilize electret materials (materials with permanent dipoles) to induce image charges on particles, thereby enhancing particle capture. However, for particles with aerodynamic or mobility dimensions of 100 to 300 nm, mechanical capture (diffusion, impaction, and interception) becomes ineffective.

It is noteworthy that optical particle counters were employed as detectors in the ASTM F2299 test method. The light scattering effectiveness of small particles decreases rapidly with particle size, leading to a compromised responsiveness of optical particle counters for smaller particles. Consequently, the sensitivity of optical particle counters used for particle filtration efficiency testing must be periodically validated and tested.

The effects of residual particles and multiply charged particles on the particle filtration efficiency of a face mask were investigated in this study. Based on the ASTM F2299 test method, this study utilized a

PSL particle (Thermo Scientific TMDri-CalTM) with a diameter of 100 nm and a geometric standard deviation of approximately 1.6%. The scanning mobility particle sizer (SMPS) was employed to measure the size distribution of PSL particles both upstream and downstream of the test face mask, thereby determining the particle filtration efficiency of the face mask for residual particles and multiply charged particles at various PSL particle-to-DI water ratios. The PSL particle-to-DI water ratios employed in this investigation were 10, 20, and 100 drops per 200 mL, respectively.

Results obtained from the study revealed that PSL suspension residual particles with a mobility diameter less than 60 nanometers, as well as multiple charged particles with a mobility diameter exceeding 100 nanometers, were discovered to introduce complexity to purportedly monodisperse particle aerosols. As the PSL concentration in suspension was increased, the prominence of the residual peak became more pronounced. At higher concentrations, PSL multiply charged particles became discernible in the size distribution.

The particle filtration efficiency of the test face mask was determined to be approximately 99.03%, 96.77%, 96.77%, and 96.21% for blank water, 10 drop/200 mL, 20 drop/200 mL, and 100 drop/200 mL, respectively. Furthermore, it was observed that as the PSL particle-to-blank water ratios increased, the particle filtration efficiency of the test filter declined for both single charged particles and multiply charged particles (+1, +3, +4, and +5). At 10 drop/200 mL, the particle filtration efficiency of the test filter was approximately 99.41%, 99.46%, and 98.53% for +1, +1 - +5, and +1 - +5 and residual particles, respectively. For a 20-drop/200 mL sample, the particle filtration efficiency of the test face mask was approximately 98.89%, 98.84%, and 98.13% for particles with a concentration of +1, +1 - +5, and +1 - +5, respectively, while the residual particle concentration was measured. Similarly, for a 100-drop/200 mL sample, the particle filtration efficiency was approximately 98.06%, 98.66%, and 98.02% for particles with the same concentrations. The findings of this experiment will be instrumental in refining the methodology for determining the filtration efficiency of PSL particles in medical face masks.

5. Acknowledgments

This project is funded by National Research Council of Thailand (NRCT), Research contract no. N72A660662.

6. References

[1] K. O'Dowd, K. M. Nair, P. Forouzandeh, S. Mathew, J. Grant, R. Moran, J. Bartlett, J. Bird and S. C Pillai, "Face Masks and Respirators in the Fight against the COVID-19 Pandemic: A Review of Current Materials, Advances and Future Perspectives," *materials*, vol. 13, no. 15, 2020, Art. no. 3363, doi: 10.3390/ma13153363.

[2] C. M Dugdale and R. P. Walensky, "Filtration Efficiency, Effectiveness, and Availability of N95 Face Masks for COVID-19 Prevention," JAMA Internal Medicine, vol. 180, no. 12, 2020, Art. no. 1612, doi: 10.1001/jamainternmed.2020.4218

[3] *COVID - 19 situation report*, Department of Disease Control Thailand, Aug. 2021. [Online]. Available: https://covid19.ddc.moph.go.th/.

[4] P. Intra, "Filtration Efficiency of Surgical Masks, Fabric Masks and N95/KN95/FFP1/FFP2 Masks Available for Use during the COVID-19 Pandemic in Thailand," *Thai Science and Technology Journal*, vol. 29, no. 5, pp. 904–918, 2021, doi: 10.14456/tstj.2021.76.

[5] *Standard Test Method: Determining the Initial Efficiency of Materials Used in Medical face masks to Penetration by Particulates Using Latex Spheres*, ASTM F2299/F2299M-03, ASTM International, West Conshohocken, PA, USA, Feb. 16, 2024. [Online]. Available: https://www.astm.org/f2299_f2299m-03r17.html.

[6] *Standard Specification for Performance of Materials Used in Medical Face Masks*, ASTM F2100-19e01, ASTM International, West Conshohocken, PA, USA, Dec. 8, 2020. [Online]. Available: https://www.astm.org/f2100-19e01.html.

[7] W. John, "Size Distribution Characteristics of Aerosols," in *Aerosol Measurement: Principles, Techniques and Applications*, P. Kulkarni, P. A. Baron and K. WILLEKE, Eds, 3rd ed. Hoboken, NJ, USA: John Wiley & Sons, Inc., 2011, ch. 4, sec.4.2, pp. 45–46.

[8] S. H. R. A. Mazhar, "Relative Bio-Equivalence of Salbutamol MDIs Without and With the attached Spacers," Ph.D. dissertation, School of Pharmacy and Medical Sci., Bradford Univ., Bradford, UK, 2018.

[9] W. Yim, Cheng, S. H. Patel, R. Kou, Y. S. Meng and J. V. Jokerst, "KN95 and N95 Respirators Retain Filtration Efficiency despite a Loss of Dipole Charge during Decontamination," *ACS Applied Materials & Interfaces*, vol. 12, no. 49, pp. 54473–54480, 2020, doi: 10.1021/acsami.0c17333.

[10] S. Rengasamy, A, Miller and BC, Eimer, "Evaluation of the filtration performance of NIOSH - approved N95 filtering facepiece respirators by photometric and number - based test methods," *Journal of Occupational and Environmental Hygiene*, vol. 8, no. 1, pp. 23–30, 2011, doi: 10.1080/15459624.2010.515556.